JHEP

Published for SISSA by Springer

Received: *March 10, 2016*
Accepted: *April 13, 2016*
Published: *May 4, 2016*

CP-violation in the ZZZ and ZWW vertices at e^+e^- colliders in Two-Higgs-Doublet Models

B. Grzadkowski,[a] **O.M. Ogreid**[b] **and P. Osland**[c]

[a] *Faculty of Physics, University of Warsaw, Pastura 5, 02-093 Warsaw, Poland*
[b] *Bergen University College, Postboks 7030, N-5020 Bergen, Norway*
[c] *Department of Physics, University of Bergen, Postboks 7803, N-5020 Bergen, Norway*

E-mail: bohdan.grzadkowski@fuw.edu.pl, omo@hib.no, Per.Osland@ift.uib.no

Abstract: We discuss possibilities of measuring CP violation in the Two-Higgs-Doublet Model by studying effects of one-loop generated ZZZ and ZWW vertices. We discuss a set of CP-sensitive asymmetries for ZZ and W^+W^- production at linear e^+e^--colliders, that directly depends on the weak-basis invariant $\mathrm{Im}\, J_2$ that parametrises the strength of CP violation. Given the restrictions on this model that follow from the LHC measurements, the predicted effects are small. Pursuing such measurements is however very important, as an observed signal might point to a richer scalar sector.

Keywords: Beyond Standard Model, CP violation, Higgs Physics

ArXiv ePrint: 1603.01388

Open Access, © The Authors.
Article funded by SCOAP[3].

doi:10.1007/JHEP05(2016)025

JHEP05(2016)025

Contents

1 Introduction

Anomalous contributions to trilinear electroweak vector boson couplings have been thoroughly studied [1–5] and searched for, at LEP [6], at Fermilab [7–10] and at the LHC [11–21]. Experimentally, the

$$VW^+W^-, \quad V = \gamma, Z \tag{1.1}$$

couplings are considered the more accessible, whereas the

$$VZZ, \quad V = \gamma, Z \tag{1.2}$$

JHEP05(2016)025

couplings are considered more challenging. Both classes may have a CP-violating, as well as a CP-conserving part.

In the Standard Model (SM), at the tree level, only the γWW and ZWW couplings are non-zero, whereas all four receive contributions at the one-loop level. In the SM, CP-violating effects can only be induced via the CKM matrix. However, at one-loop order, there is no such contribution, since there might be only two relatively complex-conjugated $\bar{q}q'W$ vertices, hence CP-violating phases of the CKM matrix would cancel. An extended Higgs sector may naturally modify this at the one-loop level, since new sources of CP violation could enter in a non-trivial way.

As is well known, the Two-Higgs-Doublet Model allows for CP violation, either explicit or spontaneous [22]. Early work on CP violation in the Higgs sector related it to the couplings of neutral scalars to the electroweak gauge bosons, as well as to the charged scalars [23, 24]. The conditions for having CP violation in the model can be expressed in terms of three invariants, in ref. [25] denoted $\mathrm{Im}\, J_1$, $\mathrm{Im}\, J_2$ and $\mathrm{Im}\, J_3$. If any one of them is non-zero, then CP is violated [25] (see also ref. [26]). Further criteria would allow to distinguish spontaneous and explicit CP violation [25, 27].

Standard-model contributions to the ZZZ and ZWW vertices have been studied in [28] and [29], respectively. Since there is some scope for further constraining or even measuring CP violation in these couplings, we present an updated review of these observables, and also propose some new ones.

The paper is organized as follows. After a brief review of the model and the basic CP-violating invariants in section 2, we discuss one-loop contributions to the ZZZ and ZWW vertices in sections 3 and 4. Selected CP-violating asymmetries that could be measured in e^+e^- collisions are discussed in section 5, and concluding remarks are given in section 6. Technical details are relegated to appendices.

2 The model

We adopt a standard parametrization for the scalar potential of the 2HDM (see, for example, [30]) with

$$\Phi_i = \begin{pmatrix} \varphi_i^+ \\ (v_i + \eta_i + i\chi_i)/\sqrt{2} \end{pmatrix}, \quad i = 1, 2. \tag{2.1}$$

In the general CP-violating case, the model contains three neutral scalars, which are linear compositions of the η_i and χ_i:

$$\begin{pmatrix} H_1 \\ H_2 \\ H_3 \end{pmatrix} = R \begin{pmatrix} \eta_1 \\ \eta_2 \\ \eta_3 \end{pmatrix}, \tag{2.2}$$

with η_3 a linear combination of the χ_i that is orthogonal to the Goldstone field G_0. Furthermore, the 3×3 rotation matrix R satisfies

$$R\mathcal{M}^2 R^{\mathrm{T}} = \mathcal{M}^2_{\mathrm{diag}} = \mathrm{diag}(M_1^2, M_2^2, M_3^2), \tag{2.3}$$

where $\mathcal{M}^2$ is the neutral-sector mass-squared matrix, and with $M_1 \leq M_2 \leq M_3$.

The weak-basis invariants revealing CP violation were originally expressed by Lavoura, Silva and Botella [23, 24], in terms of couplings and rotation-matrix elements. The notation

JHEP05(2016)025

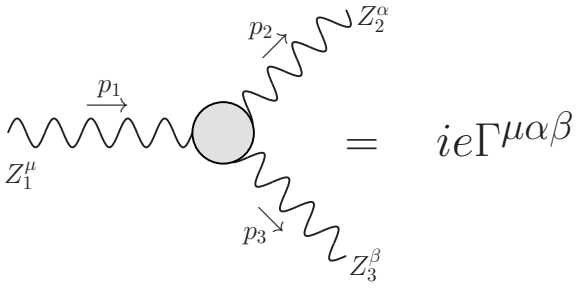

Figure 1. The general ZZZ vertex.

$\mathrm{Im}\, J_i$, where the invariants were expressed in terms of potential parameters was introduced by Gunion and Haber [25]. It was recently discussed in more detail by the present authors [30] (where also $\mathrm{Im}\, J_3$ was replaced by another related invariant which we named $\mathrm{Im}\, J_{30}$). The invariant $\mathrm{Im}\, J_2$, which represents CP violation in the mass matrix, can be written as

$$\begin{aligned}\mathrm{Im}\, J_2 &= \frac{2e_1e_2e_3}{v^9}(M_1^2 - M_2^2)(M_2^2 - M_3^2)(M_3^2 - M_1^2) \\ &= \frac{2e_1e_2e_3}{v^9}\sum_{i,j,k}\epsilon_{ijk}M_i^4M_k^2,\end{aligned} \tag{2.4}$$

where M_i are the neutral Higgs masses, and $e_i \equiv v_1R_{i1} + v_2R_{i2}$ represents their couplings to a Z or a W (for a full dictionary of couplings determined by e_i, see appendix B of ref. [30]).

We shall in this paper focus on processes in which $\mathrm{Im}\, J_2$ is responsible for the CP violation. This invariant is the only one which does not involve charged scalars. Charged scalars are involved in processes for which $\mathrm{Im}\, J_1$ and/or $\mathrm{Im}\, J_{30}$ are responsible for the CP violation. For the explicit form of these invariants and processes to which they contribute, we refer to ref. [30].

3 The ZZZ vertex

One of the simplest vertex functions to which $\mathrm{Im}\, J_2$ contributes, is the effective ZZZ vertex discussed in appendix A. Since each ZH_iH_j vertex contains a factor ϵ_{ijk} (see appendix B of ref. [30]), it follows that i, j, k must be some permutation of $1, 2, 3$ and thus an over-all factor of $e_1e_2e_3$ will emerge.

CP-violating form factors for triple gauge boson couplings have previously been studied in the 2HDM in refs. [31–33].

3.1 Lorentz structure

Phenomenological discussions [2–5] of the ZZZ vertex have presented its most general Lorentz structure. In ref. [4] the CP-violating vertex is analyzed, with all Z_1, Z_2, Z_3 off-shell. A total of 14 Lorentz structures are identified, all preserving parity. Some of these vanish when one or more Z is on-shell. (For a detailed discussion of this structure, see ref. [34].) We characterize them by momenta and Lorentz indices (p_1, μ), (p_2, α) and

JHEP05(2016)025

(p_3, β), and let Z_1 be off-shell while Z_2 and Z_3 are on-shell. In addition, we assume that Z_1 couples to a pair of leptons e^+e^- and neglect terms proportional to the lepton mass. Then according to [3] the structure reduces to the form.[1]

$$e\Gamma^{\alpha\beta\mu}_{ZZZ} = ie\frac{p_1^2 - M_Z^2}{M_Z^2}\left[f_4^Z(p_1^\alpha g^{\mu\beta} + p_1^\beta g^{\mu\alpha}) + f_5^Z \epsilon^{\mu\alpha\beta\rho}\ell_\rho\right], \tag{3.1}$$

where

$$\ell \equiv p_2 - p_3 \equiv 2p_2 - p_1 \tag{3.2}$$

with e being the proton charge, the momenta (p_1 incoming and p_2, p_3 outgoing) and Lorentz indices as defined in figure 1. The dimensionless form factor f_4^Z violates CP while f_5^Z conserves CP.

Our aim is to determine the CP-violating contributions to the ZZZ vertex, hence the contributions to f_4^Z. Let us here make some qualitative comments. Summing over i, j, k (see figure 12 in appendix A) one might think that contributions to the triangle diagram would pairwise cancel because of the factor ϵ_{ijk}. Indeed, the scalar triangle diagrams do sum to zero, but there are non-vanishing tensor contributions, due to the momentum factors at the ZH_iH_j vertices.

Three classes of Feynman diagrams give contributions to the effective CP-violating ZZZ vertex, all proportional to $\mathrm{Im}\, J_2$. They are triangle diagrams with $H_iH_jH_k$ along the internal lines, as well as diagrams where one neutral Higgs boson is replaced by a neutral Goldstone G_0 field, or a Z,

$$f_4^Z = f_4^{Z,HHH} + f_4^{Z,HHG} + f_4^{Z,HHZ}. \tag{3.3}$$

These three contributions are calculated in appendix A.

3.2 Results

The total one-loop contribution to f_4^Z for the ZZZ vertex calculated in appendix A is given by a linear combination of the three-point tensor coefficient functions C_{001} and C_1 (we adopt the LoopTools notation [35]) of various arguments,

$$\begin{aligned} f_4^Z(p_1^2) = {} & \frac{2\alpha}{\pi \sin^3(2\theta_W)}\frac{M_Z^2}{p_1^2 - M_Z^2}\frac{e_1e_2e_3}{v^3} \\ & \times \sum_{i,j,k}\epsilon_{ijk}\big[C_{001}(p_1^2, M_Z^2, M_Z^2, M_i^2, M_j^2, M_Z^2) + C_{001}(p_1^2, M_Z^2, M_Z^2, M_Z^2, M_j^2, M_k^2) \\ & + C_{001}(p_1^2, M_Z^2, M_Z^2, M_i^2, M_Z^2, M_k^2) - C_{001}(p_1^2, M_Z^2, M_Z^2, M_i^2, M_j^2, M_k^2) \\ & + M_Z^2 C_1(p_1^2, M_Z^2, M_Z^2, M_i^2, M_Z^2, M_k^2)\big]. \end{aligned} \tag{3.4}$$

This structure was identified 20 years ago by Chang, Keung and Pal [32], who studied the set of diagrams presented in appendices A.1 and A.2. We find numerically that our

[1] Here, we follow the convention of Hagiwara et al. [2], which we also adopt in section 4 for the ZWW vertex by putting $\epsilon_{0123} = -\epsilon^{0123} = +1$, whereas Gounaris et al. [3] have chosen the convention where $\epsilon^{0123} = +1$.

JHEP05(2016)025

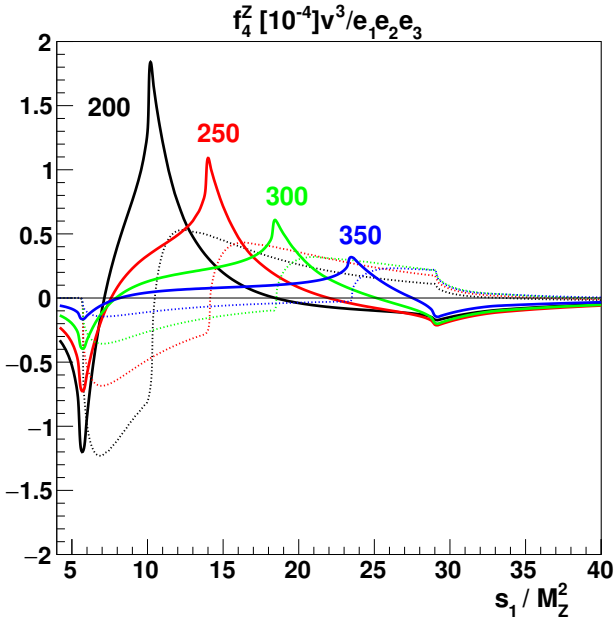

Figure 2. Real (solid lines) and imaginary (dashed) part of the form factor f_4^Z (divided by $e_1e_2e_3/v^3$) as a function of p_1^2/M_Z^2, for $p_2^2 = p_3^2 = M_Z^2$ and four values of neutral-Higgs masses M_2 of eq. (3.5), as indicated (in GeV). Below threshold, $s_1 = p_1^2 = 4M_Z^2$, the function is not defined.

result for the sum of these diagrams is identical to their result. There are, however, also diagrams with an internal Z line, arising from the ZZH_i vertex which was not included in their study. These contributions are calculated in appendix A.3, and numerical studies show that these are actually the dominant contributions.

For the neutral-Higgs masses

$$M_1 = 125 \text{ GeV}, \quad M_2 = (200, 250, 300, 350) \text{ GeV}, \quad M_3 = 400 \text{ GeV}, \tag{3.5}$$

we show in figure 2 the value of $f_4^Z(p_1^2)v^3/(e_1e_2e_3)$ as a function of p_1^2/M_Z^2. The normalization factor, $e_1e_2e_3/v^3$, is typically of $\mathcal{O}(0.1)$ (only small regions of the parameter space are compatible with theoretical and experimental constraints [36, 37]). Defining δ as a measure of deviation of the H_1VV coupling from its SM strength, $e_1 = v(1-\delta)$, and using $e_2^2 + e_3^2 = v^2 - e_1^2$, one can easily find [30] that for small δ, $(e_1e_2e_3)/v^3 < \delta$, so it is suppressed by the H_1VV coupling approaching the SM limit.

The form factor f_4^Z has been constrained by experiments at LEP, Fermilab and the LHC. Recently, CMS [20] has presented an impressive bound on f_4^Z (assumed real): $-0.0022 < f_4^Z < 0.0026$. This result is obtained in the $2\ell 2\nu$ channel from the 7 and 8 TeV data sets. It is still two orders of magnitude above what is generated in the 2HDM by a non-zero Im J_2.

JHEP05(2016)025

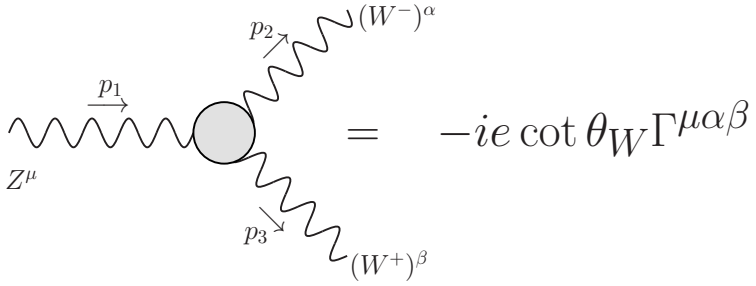

$$= \quad -ie\cot\theta_W\Gamma^{\mu\alpha\beta}$$

Figure 3. The general ZWW vertex.

4 The ZW^+W^- vertex

Contrary to the ZZZ vertex, the ZWW vertex is present at the tree level, with a well-known, CP-conserving structure:

$$ig_{ZWW}\Gamma^{\alpha\beta\mu}_{\text{tree}} = -ig\cos\theta_W[g^{\alpha\beta}(p_2-p_3)^\mu + g^{\beta\mu}(p_1+p_3)^\alpha - g^{\mu\alpha}(p_1+p_2)^\beta] \tag{4.1a}$$

$$= -ig\cos\theta_W\left[g^{\alpha\beta}\ell^\mu + g^{\beta\mu}\left(-\frac{1}{2}\ell+\frac{3}{2}p_1\right)^\alpha - g^{\mu\alpha}\left(\frac{1}{2}\ell+\frac{3}{2}p_1\right)^\beta\right], \tag{4.1b}$$

where $g_{ZWW} = -e\cot\theta_W$, p_1 is incoming while p_2 and p_3 are outgoing, and in the second line, we make use of $\ell = p_2 - p_3$.

Triangle diagrams discussed in appendix B contribute to the CP-violating ZW^+W^- vertex. In fact, they give a contribution proportional to the invariant $\text{Im}\, J_2$, which is one measure of CP violation in the Two-Higgs-Doublet model [25] (referred to as J_1 in earlier work by Lavoura, Silva and Botella [23, 24]).

4.1 Lorentz structure

Phenomenological discussions [2] of the ZWW vertex have presented its most general Lorentz structure. We let Z be off-shell while both $W^\pm$ are on-shell, again assuming that Z couples to a pair of leptons e^+e^- so that we may neglect terms proportional to the lepton mass. Then according to [2] the structure reads

$$\begin{aligned}\Gamma^{\alpha\beta\mu}_{ZWW} = {} & f_1^Z\ell^\mu g^{\alpha\beta} - \frac{f_2^Z}{M_W^2}\ell^\mu p_1^\alpha p_1^\beta + f_3^Z\left(p_1^\alpha g^{\mu\beta} - p_1^\beta g^{\mu\alpha}\right) \\ & + if_4^Z\left(p_1^\alpha g^{\mu\beta} + p_1^\beta g^{\mu\alpha}\right) + if_5^Z\epsilon^{\mu\alpha\beta\rho}\ell_\rho \\ & - f_6^Z\epsilon^{\mu\alpha\beta\rho}p_{1\rho} - \frac{f_7^Z}{M_W^2}\ell^\mu\epsilon^{\alpha\beta\rho\sigma}p_{1\rho}\ell_\sigma.\end{aligned} \tag{4.2}$$

The tree-level vertex contributes to f_1 and f_3:

$$f_1^{\text{tree}} = 1, \quad f_3^{\text{tree}} = 2. \tag{4.3}$$

The dimensionless form factors f_4^Z, f_6^Z and f_7^Z violate CP while the others conserve CP. Recent LHC experiments [17, 19, 21] have constrained the CP-conserving anomalous couplings, but not the CP-violating f_4^Z.

JHEP05(2016)025

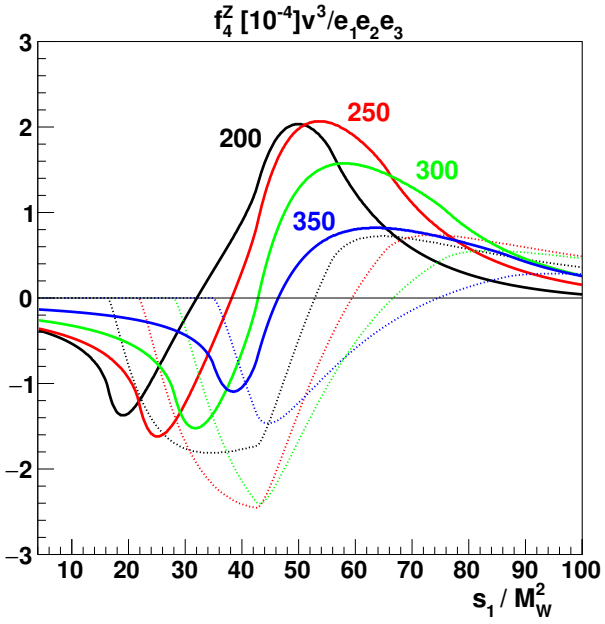

Figure 4. Real (solid lines) and imaginary (dashed) part of the form factor f_4^Z (divided by $e_1e_2e_3/v^3$) as a function of s_1/M_W^2, for $p_2^2 = p_3^2 = M_W^2$ and four values of neutral-Higgs M_2 masses of eq. (3.5), as indicated (in GeV).

Our aim is to determine the CP violating contributions to the ZWW vertex, hence the contributions to f_4^Z.

4.2 Results

The total one-loop contribution to f_4^Z for the ZWW vertex calculated in appendix B is given by a linear combination of the three-point tensor coefficient functions C_{001} of various arguments,

$$f_4^Z\left(p_1^2\right) = \frac{-\alpha}{\pi \sin^2(2\theta_{\rm W})}\frac{e_1e_2e_3}{v^3}\sum_{i,j,k}\epsilon_{ijk}\big[C_{001}(p_1^2, M_W^2, M_W^2, M_i^2, M_j^2, M_W^2) - C_{001}(p_1^2, M_W^2, M_W^2, M_i^2, M_j^2, M_{H^\pm}^2)\big]. \tag{4.4}$$

This quantity was also studied by He, Ma and McKellar [31]. Assuming that they have used the $(-i\epsilon)$ prescription in their eq. (5), we find numerical agreement apart from an overall sign. Furthermore, the result for the imaginary part given in their eq. (6) is twice as large as the one in eq. (5).

For the neutral-Higgs masses given by equation (3.5), we show in figure 4 the value of $f_4^Z(p_1^2)v^3/(e_1e_2e_3)$ as a function of s_1/M_W^2.

5 Asymmetries

We are going to discuss the possibility of testing CP violation at future e^+e^- colliders [38, 39]. It is assumed that polarizations of the final-state vector bosons could be determined

JHEP05(2016)025

experimentally.[2] We adopt CP-sensitive observables defined for W^+W^- and ZZ in [33, 40], and [32], respectively. Below, we present some predictions for those and other asymmetries for the 2HDM.

5.1 $e^+e^- \to ZZ$

Helicities of the ZZ (and W^+W^-) pairs can be measured statistically by studying decay products of the final vector bosons. Therefore, we will define a number of differential asymmetries assuming that both the momenta and helicities of the ZZ pair could be determined. Since our goal is to measure the CP-violating form factor f_4^Z, our asymmetries will (to leading order) be proportional to f_4^Z. Let us first start by considering

$$A_1^{ZZ} \equiv \frac{\sigma_{+,0} - \sigma_{0,-}}{\sigma_{+,0} + \sigma_{0,-}}, \tag{5.1}$$

$$A_2^{ZZ} \equiv \frac{\sigma_{0,+} - \sigma_{-,0}}{\sigma_{0,+} + \sigma_{-,0}}, \tag{5.2}$$

where $\sigma_{\lambda,\bar{\lambda}}$ are unpolarized-beam cross sections for the production of ZZ with helicities λ and $\bar{\lambda}$, respectively. The cross sections can be expressed through the helicity amplitudes for $e^+(\sigma)e^-(\bar{\sigma}) \to Z(\lambda)Z(\bar{\lambda})$ as follows

$$\sigma_{\lambda,\bar{\lambda}} = \sum_{\sigma,\bar{\sigma}} \mathcal{M}_{\sigma,\bar{\sigma};\lambda\bar{\lambda}}(\Theta)\mathcal{M}^{\star}_{\sigma,\bar{\sigma};\lambda\bar{\lambda}}(\Theta), \tag{5.3}$$

where σ and $\bar{\sigma}$ are the helicities of e^- and e^+, respectively. Expressions for these cross sections can readily be written out using the results from Chang, Keung and Pal [32]. Letting Θ be the angle between the e^- beam direction and the Z whose helicity is given by the first index λ, and defining $\gamma = \sqrt{s_1}/(2M_Z)$ and $\beta^2 = 1 - \gamma^{-2}$, we find to lowest order in f_4^Z

$$A_1^{ZZ} = -4\beta\gamma^4 \left[(1+\beta^2)^2 - (2\beta\cos\Theta)^2\right] \mathcal{F}_1(\beta,\Theta)\,\mathrm{Im}\, f_4^Z, \tag{5.4}$$

with $\mathcal{F}_1(\beta,\Theta)$ given in appendix D.

In the low-energy limit ($\beta \to 0$) this simplifies to

$$A_1^{ZZ} = \frac{-4\beta\left[\xi_1 - 3\xi_1\cos^2\Theta + 2\left(\xi_1 - \xi_2\right)\cos^3\Theta\right]\mathrm{Im}\, f_4^Z}{\left(\xi_3+\xi_4\right) + 2\xi_3\cos\Theta - 3\left(\xi_3+\xi_4\right)\cos^2\Theta - 4\xi_3\cos^3\Theta + 4\left(\xi_3+\xi_4\right)\cos^4\Theta}, \tag{5.5}$$

where the ξ_i are given in appendix D. Furthermore, we find

$$A_2^{ZZ} = A_1^{ZZ}\left(\cos\Theta \to -\cos\Theta\right). \tag{5.6}$$

These asymmetries are both shown in figure 5. The sharp peaks near the forward and backward directions are due to an interplay of three factors: (1) the near-divergence of the t-channel propagator, (2) the factor $[\Delta\sigma\Delta\lambda(1+\beta^2) - 2\cos\Theta]$ of the amplitude (see eq. (5) in ref. [32]) and (3) the Wigner functions proportional to $1 \pm \cos\Theta$.

[2] Investigating angular distributions of the vector boson decay products one can indeed measure their polarizations.

JHEP05(2016)025

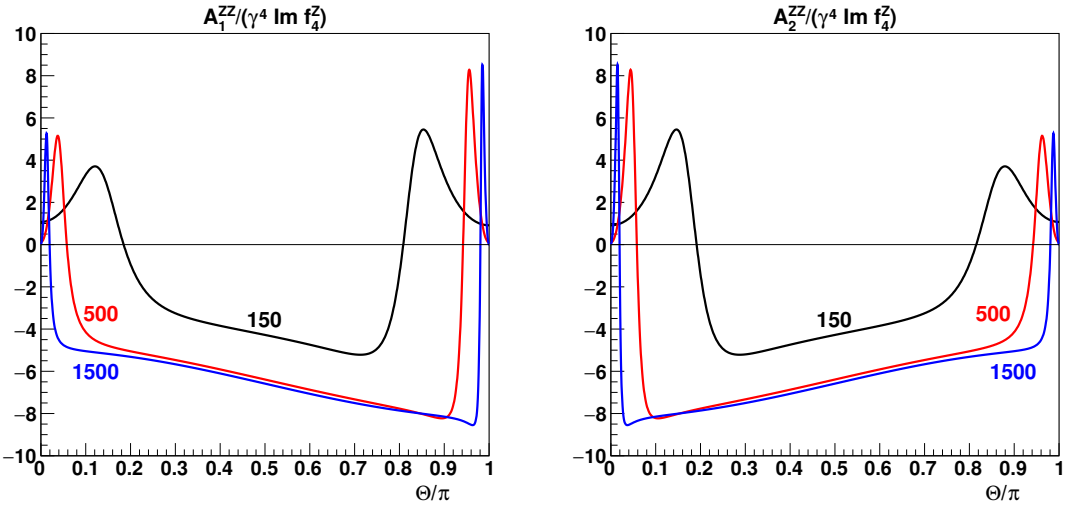

Figure 5. The asymmetries $A_1^{ZZ}(\Theta)$ of eq. (5.4) and $A_2^{ZZ}(\Theta)$ of eq. (5.6)(both divided by $\gamma^4\,\mathrm{Im}\,f_4^Z$) as functions of Θ for three beam energies E as indicated (in GeV).

Introducing the abbreviations

$$\xi = \frac{2\sin\theta_W\cos\theta_W(1-6\sin^2\theta_W+12\sin^4\theta_W)}{1-8\sin^2\theta_W+24\sin^4\theta_W-32\sin^6\theta_W+32\sin^8\theta_W} \simeq 1.65, \tag{5.7}$$

$$\tilde{\xi} = \frac{-4\sin\theta_W\cos\theta_W\left(1-6\sin^2\theta_W+12\sin^4\theta_W-16\sin^6\theta_W\right)}{1-8\sin^2\theta_W+24\sin^4\theta_W-32\sin^6\theta_W+32\sin^8\theta_W} \simeq -0.78, \tag{5.8}$$

the following asymmetries can be defined and calculated to leading order in f_4^Z:

$$\begin{aligned} A^{ZZ} &\equiv \frac{\sigma_{+,0}+\sigma_{0,+}-\sigma_{0,-}-\sigma_{-,0}}{\sigma_{+,0}+\sigma_{0,+}+\sigma_{0,-}+\sigma_{-,0}} \\ &= \frac{-2\beta\gamma^4[(1+\beta^2)^2-(2\beta\cos\Theta)^2][1+\beta^2-(3-\beta^2)\cos^2\Theta]\xi\,\mathrm{Im}\,f_4^Z}{(1+\beta^2)^2-(3+6\beta^2-\beta^4)\cos^2\Theta+4\cos^4\Theta}, \end{aligned} \tag{5.9}$$

$$\begin{aligned} \tilde{A}^{ZZ} &\equiv \frac{\sigma_{+,0}-\sigma_{0,+}-\sigma_{0,-}+\sigma_{-,0}}{\sigma_{+,0}+\sigma_{0,+}+\sigma_{0,-}+\sigma_{-,0}} \\ &= \frac{-2\beta\gamma^4\cos\Theta[(1+\beta^2)^2-(2\beta\cos\Theta)^2]\left(\beta^2-\cos^2\Theta\right)\tilde{\xi}\mathrm{Im}\,f_4^Z}{\left(1+\beta^2\right)^2-(3+6\beta^2-\beta^4)\cos^2\Theta+4\cos^4\Theta}. \end{aligned} \tag{5.10}$$

The asymmetries A^{ZZ} and $\tilde{A}^{ZZ}$ are both shown in figure 6 for three values of the energy. Since the former is defined symmetrically with respect to the two Z bosons, the expression is forward-backward symmetric. At high energies and intermediate angles, it is well approximated by $A^{ZZ} \simeq -4\gamma^4\xi\,\mathrm{Im}\,f_4^Z$.

In the low-energy limit, these become

$$A^{ZZ} \to \frac{-2\beta(1-3\cos^2\Theta)\xi\,\mathrm{Im}\,f_4^Z}{1-3\cos^2\Theta+4\cos^4\Theta}, \tag{5.11}$$

$$\tilde{A}^{ZZ} \to \frac{2\beta\cos^3\Theta\tilde{\xi}\,\mathrm{Im}\,f_4^Z}{1-3\cos^2\Theta+4\cos^4\Theta}. \tag{5.12}$$

JHEP05(2016)025

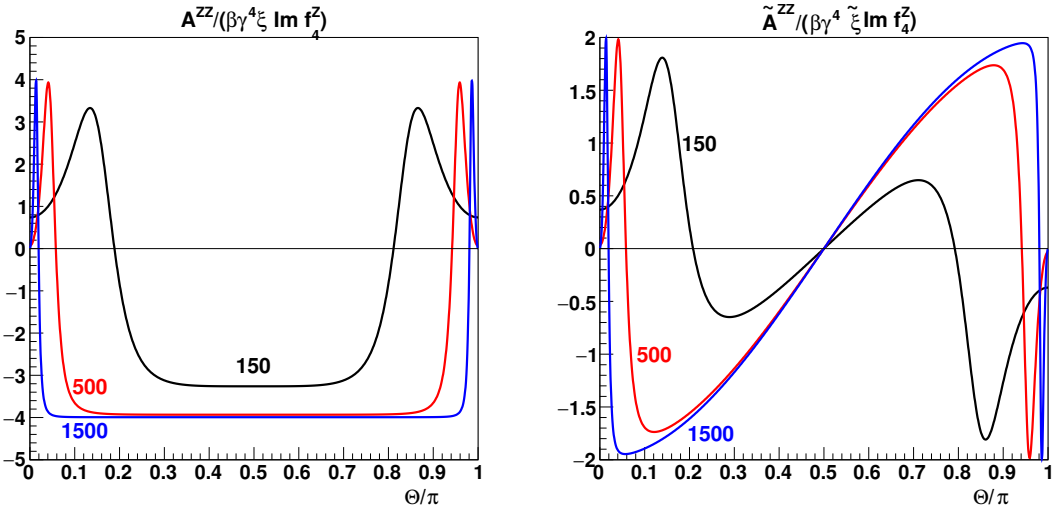

Figure 6. The asymmetries $A^{ZZ}(\Theta)$ and $\tilde{A}^{ZZ}(\Theta)$ of eqs. (5.9) and (5.10) (divided by $\beta\gamma^4\xi\,\mathrm{Im}\,f_4^Z$ and $\beta\gamma^4\tilde{\xi}\,\mathrm{Im}\,f_4^Z$) and as functions of Θ for three beam energies E as indicated (in GeV).

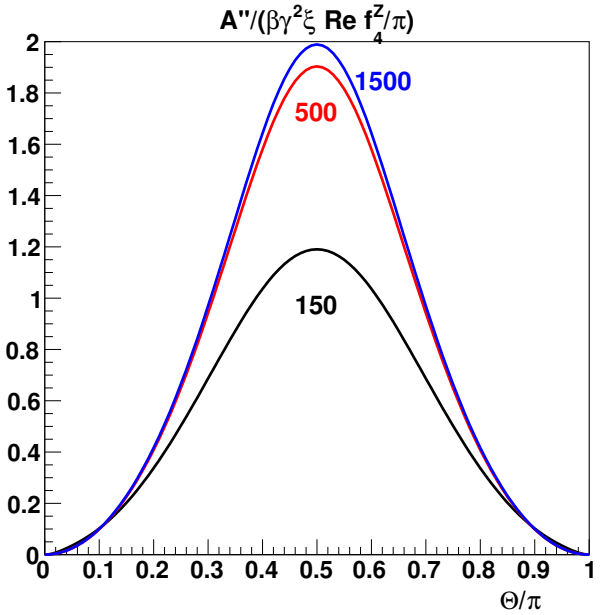

Figure 7. The asymmetry $\mathcal{A}''(\Theta)$ of eq. (5.15) (divided by $\beta\gamma^2\xi\,\mathrm{Re}\,f_4^Z/\pi$) as a function of Θ for three beam energies E as indicated (in GeV).

Other possibilities of testing CP violation in $e^+e^- \to ZZ$ have been investigated by Chang, Keung and Pal [32], who note that the angular distribution of ℓ^- from a Z decay is determined by the spin-density matrix of the Z (see eq. (10) of ref. [32]):

$$\rho(\Theta)_{\lambda_1\lambda_2} = \mathcal{N}^{-1}(\Theta) \sum_{\sigma,\bar{\sigma},\bar{\lambda}} \mathcal{M}_{\sigma,\bar{\sigma},\lambda_1,\bar{\lambda}}(\Theta)\mathcal{M}^*_{\sigma,\bar{\sigma},\lambda_2,\bar{\lambda}}(\Theta). \tag{5.13}$$

where again, σ and $\bar{\sigma}$ are helicities of e^- and e^+, respectively, and the λ and $\bar{\lambda}$ refer to the two Z helicities. They advocate a certain difference of cross sections, integrated over

JHEP05(2016)025

azimuthal quadrants of the final-state leptons, which is not suppressed by the approximate C-symmetry. They have thus defined such a "folded" asymmetry $\mathcal{A}''(\Theta)$ in their eq. (15), and shown that it equals

$$\mathcal{A}''(\Theta) = -\frac{1}{\pi}\left[\mathrm{Im}\,\rho(\Theta)_{+,-} - \mathrm{Im}\,\rho(\pi-\Theta)_{-,+}\right]. \tag{5.14}$$

To lowest order in f_4^Z, this quantity is proportional to $\mathrm{Re}\, f_4^Z$:

$$\mathcal{A}''(\Theta) = \frac{\beta(1+\beta^2)\gamma^2[(1+\beta^2)^2 - (2\beta\cos\Theta)^2]\sin^2\Theta\,\xi\,\mathrm{Re}\, f_4^Z}{\pi[2+3\beta^2-\beta^6-\beta^2(9-10\beta^2+\beta^4)\cos^2\Theta - 4\beta^4\cos^4\Theta]}. \tag{5.15}$$

This asymmetry is shown in figure 7 for three values of the energy. Superficially, it looks like this asymmetry might be unbounded at high energies. This is not the case, since at high energies (see appendix C) f_4^Z falls off like $(1/\gamma^6)\log\gamma$.

In the low-energy limit ($\beta \to 0$), it simplifies:

$$\mathcal{A}''(\Theta) \to \frac{\beta\sin^2\Theta\,\xi\,\mathrm{Re}\, f_4^Z}{2\pi}. \tag{5.16}$$

5.2 $e^+e^- \to W^+W^-$

Let us follow the same approach as for $e^+e^- \to ZZ$ in the $e^+e^- \to W^+W^-$ case by forming the asymmetries [33]:

$$A_1^{WW} \equiv \frac{\sigma_{+,0} - \sigma_{0,-}}{\sigma_{+,0} + \sigma_{0,-}}, \tag{5.17}$$

$$A_2^{WW} \equiv \frac{\sigma_{0,+} - \sigma_{-,0}}{\sigma_{0,+} + \sigma_{-,0}}, \tag{5.18}$$

where $\sigma_{\lambda,\bar\lambda}$ are unpolarized-beam cross sections for the production of W^- and W^+ with helicities λ and $\bar\lambda$, respectively. The cross sections can be expressed through the helicity amplitudes for $e^+(\sigma)e^-(\bar\sigma) \to W^-(\lambda)W^+(\bar\lambda)$ like in eq. (5.3), where σ and $\bar\sigma$ are the helicities of e^- and e^+, respectively. The amplitudes $\mathcal{M}_{\sigma,\bar\sigma;\lambda\bar\lambda}(\Theta)$ were first calculated in [2]. Here, Θ is the angle between the e^- and the W^- momenta.

Following the notation of [33], we find for the case of polarized initial beams $(\sigma,\bar\sigma)$, and to lowest order in f_4^Z:

$$(\sigma,\bar\sigma) = (+-): \quad A_1^{WW} = \frac{s_1}{M_Z^2}\mathrm{Im}\, f_4^Z, \tag{5.19a}$$

$$(\sigma,\bar\sigma) = (-+): \quad A_1^{WW} = \frac{-\beta^2(1-2\sin^2\theta_W)s_1}{\beta^2(2\sin^2\theta_W M_Z^2 - s_1) + (s_1 - M_Z^2)Y}\mathrm{Im}\, f_4^Z, \tag{5.19b}$$

where

$$Y \equiv 1 - \frac{(1+\beta)}{\gamma^2(1+\beta^2-2\beta\cos\Theta)}. \tag{5.20}$$

with $\gamma = \sqrt{s_1}/(2M_W)$ and $\beta^2 = 1-\gamma^{-2}$.

For the unpolarized case, we find (still to lowest order in f_4^Z):

$$A_1^{WW} = \frac{N_1^{(a)}(1-\cos\Theta)^2 + N_1^{(b)}(1+\cos^2\Theta)}{D_1^{(a)}(1-\cos\Theta)^2 + D_1^{(b)}(1+\cos^2\Theta)}\,\beta s_1\,\mathrm{Im}\, f_4^Z \tag{5.21}$$

JHEP05(2016)025

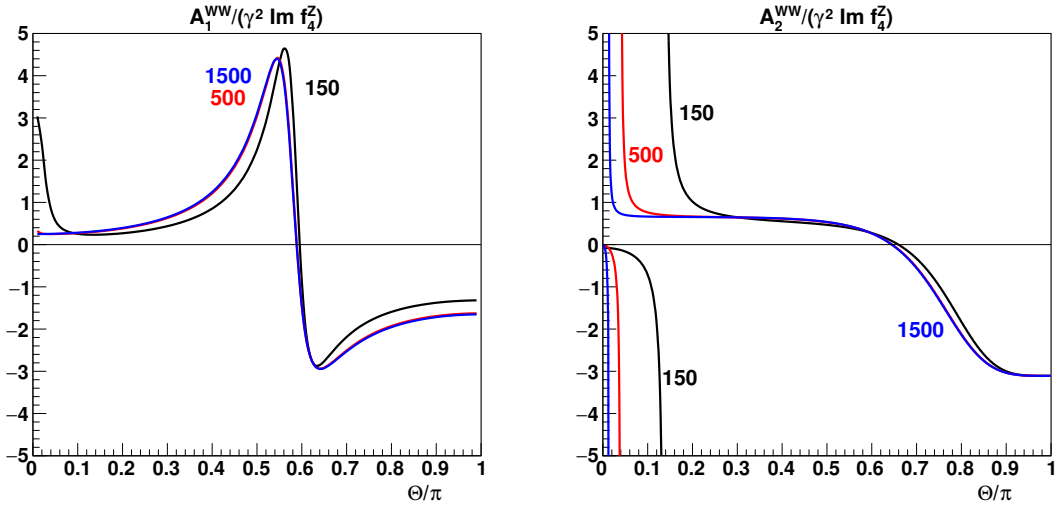

Figure 8. The asymmetries A_1^{WW} and A_2^{WW} vs Θ for three values of the beam (or W) energy E, 150 GeV, 500 GeV and 1500 GeV, as indicated.

with the following abbreviations:

$$N_1^{(a)} = (1+\beta^2-2\beta\cos\Theta)\{X_1 - 2\sin^2\theta_W[(1-\beta^2)(1-\beta+2\cos\Theta)s_1 - (1-3\beta-\beta^2+2\beta^2\cos\Theta-\beta^3+2\cos\Theta)M_Z^2]\}, \tag{5.22a}$$

$$N_1^{(b)} = 8\sin^4\theta_W\beta(1+\beta^2-2\beta\cos\Theta)^2M_Z^2, \tag{5.22b}$$

$$D_1^{(a)} = X_1^2 - 4\sin^2\theta_W\beta(1+\beta^2-2\beta\cos\Theta)X_1M_Z^2, \tag{5.22c}$$

$$D_1^{(b)} = 8\sin^4\theta_W\beta^2(1+\beta^2-2\beta\cos\Theta)^2M_Z^4, \tag{5.22d}$$

$$X_1 = (1-\beta^2)(1-\beta+2\cos\Theta)s_1 - (1-2\beta-\beta^2+2\cos\Theta)M_Z^2. \tag{5.22e}$$

In the low-energy limit ($\beta \to 0$), this simplifies:

$$A_1^{WW} \to \begin{cases} \frac{4M_W^2}{M_Z^2}\frac{2M_W^2-M_Z^2}{(4M_W^2-M_Z^2)(1+2\cos\Theta)}\beta\,\mathrm{Im}\,f_4^Z, & \beta \lesssim |1+2\cos\Theta|, \quad \beta \ll 1, \\ -\frac{2M_W^2\left(16M_W^4-5M_W^2M_Z^2-2M_Z^4\right)}{M_Z^2\left(10M_W^4-2M_W^2M_Z^2+M_Z^4\right)}\,\mathrm{Im}\,f_4^Z, & |1+2\cos\Theta| \lesssim \beta \ll 1, \end{cases} \tag{5.23}$$

where we have also substituted the tree-level relation $\sin^2\theta_W = 1 - M_W^2/M_Z^2$.

Furthermore, we find

$$A_2^{WW} = -A_1^{WW}\,(\cos\Theta \to -\cos\Theta; \beta \to -\beta)\,. \tag{5.24}$$

We display these asymmetries A_1^{WW} and A_2^{WW} in figure 8. An overall factor $\gamma^2\,\mathrm{Im}\,f_4^Z$ is factored out, and hence for A_1^{WW}, the graphs for 500 GeV and 1500 GeV are practically indistinguishable. The main structure is due to the first term in the numerator of eq. (5.17) passing through zero close to a minimum of the denominator.

We may also combine these two asymmetries into one, either by addition or subtraction. Again calculating to lowest order in f_4^Z:

$$A^{WW} \equiv \frac{\sigma_{+,0}+\sigma_{0,+}-\sigma_{0,-}-\sigma_{-,0}}{\sigma_{+,0}+\sigma_{0,+}+\sigma_{0,-}+\sigma_{-,0}} = \beta\left(1+\beta^2-2\beta\cos\Theta\right)\mathcal{F}^{WW}\,\mathrm{Im}\,f_4^Z, \tag{5.25}$$

JHEP05(2016)025

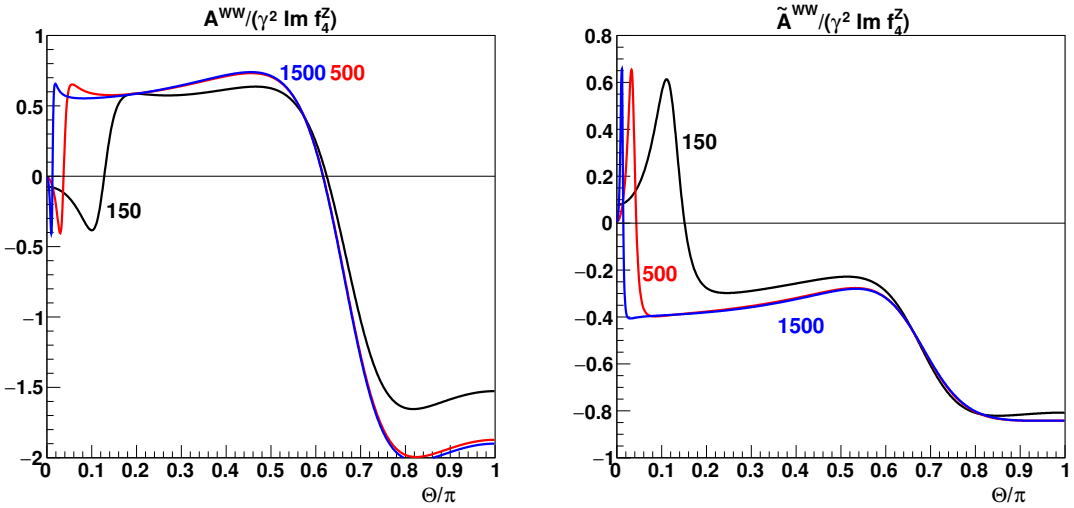

Figure 9. The asymmetries A^{WW} and $\tilde{A}^{WW}$ (divided by $\gamma^2\,\mathrm{Im}\,f_4^Z$) vs Θ for three values of the beam (or W) energy E, 150 GeV, 500 GeV and 1500 GeV, as indicated.

$$\begin{aligned}\tilde{A}^{WW} &\equiv \frac{\sigma_{+,0}-\sigma_{0,+}+\sigma_{0,-}-\sigma_{-,0}}{\sigma_{+,0}+\sigma_{0,+}+\sigma_{0,-}+\sigma_{-,0}} \\ &= \beta\left(1+\beta^2-2\beta\cos\Theta\right)\tilde{\mathcal{F}}^{WW}\,\mathrm{Im}\,f_4^Z,\end{aligned} \tag{5.26}$$

where the functions $\mathcal{F}^{WW}$ and $\tilde{\mathcal{F}}^{WW}$, given in appendix D, can be expressed as ratios of polynomials in $\cos\Theta$.

A further possibility of testing CP violation in $e^+e^- \to WW$ has been investigated in [33]. Adopting the helicity amplitudes obtained there, they have defined the up-down asymmetry $\mathcal{A}^{ud}(\Theta)$ in their eq. (32), and shown that it equals

$$\mathcal{A}^{ud}(\Theta) = \frac{3}{8}\sqrt{2}\left[\mathrm{Im}\,\rho(\Theta)_{+,0} - \mathrm{Im}\,\bar{\rho}(\Theta)_{-,0} - \mathrm{Im}\,\rho(\Theta)_{-,0} + \mathrm{Im}\,\bar{\rho}(\Theta)_{+,0}\right], \tag{5.27}$$

with $\rho(\Theta)$ the spin-density matrix of the W^- boson and $\bar{\rho}(\Theta)$ the spin-density matrix of the W^+ boson, as defined by their eqs. (26) and (28). To lowest order in f_4^Z, this quantity is proportional to $\mathrm{Re}\,f_4^Z$. It is a rather complicated function, depending on the W velocity β, the angle Θ, the ratio M_Z^2/s_1, as well as $\sin^2\theta_W$. We focus on the angular dependence, and write it as

$$\mathcal{A}^{ud} = 3\beta\sqrt{1-\beta^2}(1+\beta^2-2\beta\cos\Theta)\sin\Theta\mathcal{F}(s_1,\Theta)\,\mathrm{Re}\,f_4^Z, \tag{5.28}$$

with

$$\mathcal{F}(s_1,\Theta) \equiv \frac{N_0^{ud}+N_1^{ud}\cos\Theta+N_2^{ud}\cos^2\Theta}{D_0^{ud}+D_1^{ud}\cos\Theta+D_2^{ud}\cos^2\Theta+D_3^{ud}\cos^3\Theta+D_4^{ud}\cos^4\Theta} \tag{5.29}$$

given in appendix D. The angular dependence of this asymmetry is shown in figure 10.

In the low-energy limit, $\beta \to 0$, this reduces to

$$\mathcal{A}^{ud} \to -\frac{3}{4}\beta\frac{(1-2\sin^2\theta_W)M_W^2}{4M_W^2-M_Z^2}\sin\Theta\,\mathrm{Re}\,f_4^Z. \tag{5.30}$$

JHEP05(2016)025

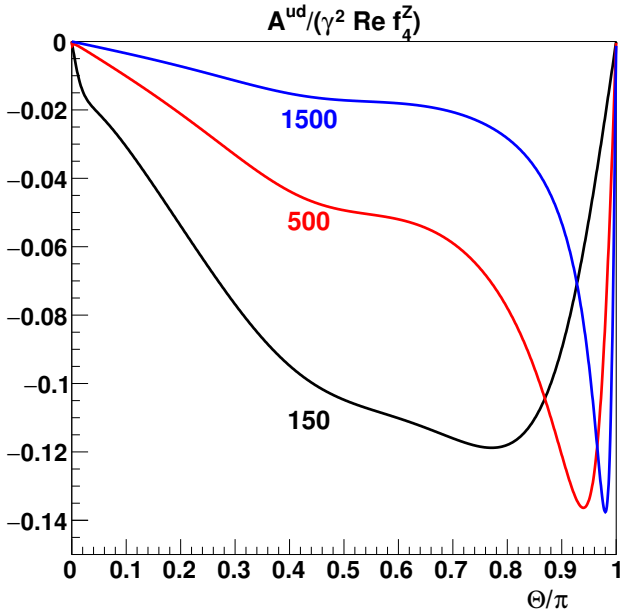

Figure 10. The asymmetry $\mathcal{A}^{ud}$ of eq. (5.28) (divided by $\gamma^2\,\mathrm{Re}\,f_4^Z$) vs Θ for three values of the beam (or W) energy E, 150 GeV, 500 GeV and 1500 GeV, as indicated.

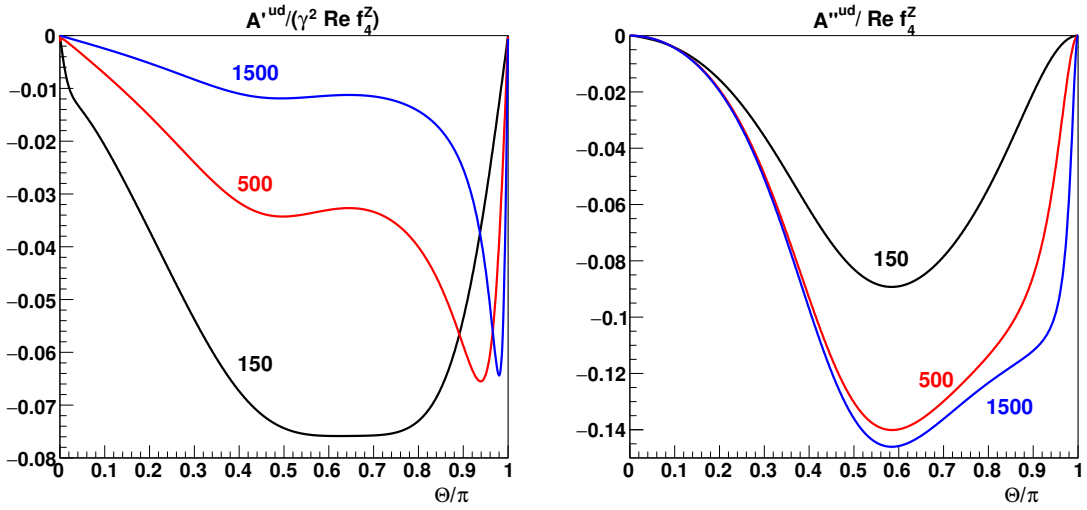

Figure 11. The asymmetries $\mathcal{A}'^{ud}$ and $\mathcal{A}''^{ud}$ divided by $\gamma^2\mathrm{Re}\,f_4^Z$ and $\mathrm{Re}\,f_4^Z$, respectively, vs Θ for three values of the beam (or W) energy E, 150 GeV, 500 GeV and 1500 GeV, as indicated. Here, $E_0 = \frac{1}{4}\sqrt{s_1}$ has been used.

On the other hand, at high energies, the prefactor $\mathcal{F}(s_1,\Theta)$ grows as γ^2 (see appendix D), but this is tempered by the high-energy fall-off of f_4^Z.

Chang, Keung and Phillips [33] have also defined an asymmetry $\mathcal{A}'^{ud}(\Theta)$ in their eq. (34), and shown that it equals

$$\mathcal{A}'^{ud} = \frac{3\sqrt{2}}{4\pi}\{[a(E_0)-b(E_0)]\,[\mathrm{Im}\,\rho(\Theta)_{+,0} - \mathrm{Im}\,\bar\rho(\Theta)_{-,0}] - [a(E_0)+b(E_0)]\,[\mathrm{Im}\,\rho(\Theta)_{-,0} - \mathrm{Im}\,\bar\rho(\Theta)_{+,0}]\}\,, \tag{5.31}$$

JHEP05(2016)025

with $a(E_0)$ and $b(E_0)$ defined in [33] following their eq. (34). To the lowest order in f_4^Z we find that

$$\mathcal{A}'^{ud} = \frac{3\beta\sqrt{1-\beta^2}(1+\beta^2-2\beta\cos\Theta)\sin\Theta\, s_1 \operatorname{Re} f_4^Z}{\pi\left(D_0^{ud}+D_1^{ud}\cos\Theta+D_2^{ud}\cos^2\Theta+D_3^{ud}\cos^3\Theta+D_4^{ud}\cos^4\Theta\right)} \times\left\{[a(E_0)-b(E_0)]\,\mathcal{N}(\beta,\cos\Theta)+[a(E_0)+b(E_0)]\,\mathcal{N}(-\beta,-\cos\Theta)\right\}, \tag{5.32}$$

where

$$\mathcal{N}(\beta,\cos\Theta) = N_0'^{ud}+N_1'^{ud}\cos\Theta+N_2'^{ud}\cos^2\Theta \tag{5.33}$$

and

$$\begin{aligned} N_0'^{ud} &= \left(1-2\beta^2-\beta^3\right)(1-\beta)^2\left(1-2\sin^2\theta_W\right)s_1 \\ &\quad -\left(1-4\beta-\beta^2+2\beta^3-2\left(1-6\beta-\beta^2+\beta^3+\beta^5\right)\sin^2\theta_W\right)m_Z^2, \qquad (5.34)\\ N_1'^{ud} &= \left(1+3\beta+2\beta^2\right)(1-\beta)^2\left(1-2\sin^2\theta_W\right)s_1 \\ &\quad -\left[(1+\beta)^2-2\left(1+3\beta+5\beta^2+\beta^3-2\beta^4\right)\sin^2\theta_W\right. \\ &\qquad \left.+8\beta\left(1+\beta^2\right)\sin^4\theta_W\right]m_Z^2, \\ N_2'^{ud} &= 2\beta^2\left(1-4\sin^2\theta_W+8\sin^4\theta_W\right)m_Z^2. \qquad (5.35) \end{aligned}$$

Finally, they have also defined

$$\mathcal{A}''^{ud} = -\frac{1}{\pi}\left(\operatorname{Im}\rho(\Theta)_{+,-}-\operatorname{Im}\bar{\rho}(\Theta)_{-,+}\right), \tag{5.36}$$

which to the lowest order in f_4^Z equals

$$\mathcal{A}''^{ud} = \frac{4\beta\left(1-\beta^2\right)^2\left(1-2\sin^2\theta_W\right)\left(1+\beta^2-2\beta\cos\Theta\right)\sin^2\Theta\left(s_1-m_Z^2\right)s_1\operatorname{Re}f_4^Z}{\pi\left(D_0^{ud}+D_1^{ud}\cos\Theta+D_2^{ud}\cos^2\Theta+D_3^{ud}\cos^3\Theta+D_4^{ud}\cos^4\Theta\right)}. \tag{5.37}$$

In the low-energy limit these become:

$$\begin{aligned} \mathcal{A}'^{ud} &= -\frac{3\beta m_W^2\left(2m_W^2-m_Z^2\right)\sin\Theta\operatorname{Re}f_4^Z}{4\pi m_Z^2\left(4m_W^2-m_Z^2\right)} \\ &\quad\times\left\{[a(E_0)-b(E_0)]\,(1+\cos\Theta)+[a(E_0)+b(E_0)]\,(1-\cos\Theta)\right\}, \qquad (5.38)\\ \mathcal{A}''^{ud} &= -\frac{\beta m_W^2\left(2m_W^2-m_Z^2\right)\sin^2\Theta\operatorname{Re}f_4^Z}{\pi m_Z^2\left(4m_W^2-m_Z^2\right)}. \qquad (5.39) \end{aligned}$$

The asymmetries $\mathcal{A}'^{ud}$ and $\mathcal{A}''^{ud}$ are shown in figure 11. Like $\mathcal{A}^{ud}$, they vary rapidly near the backward direction.

6 Discussion

The mixing of CP-even and odd components of the scalar fields lead to couplings among all pairs of neutral mass eigenstates and the gauge particles, which in turn lead to loop-induced trilinear couplings among the electroweak gauge particles, W and Z. The CP-violating part of these couplings, which we have discussed here, are all proportional to the quantity $\operatorname{Im} J_2$.

JHEP05(2016)025

This quantity $\mathrm{Im}\, J_2$ is proportional to the product of couplings $e_1 e_2 e_3$, as well as to the product of differences of masses squared, $(M_2^2 - M_1^2)(M_3^2 - M_2^2)(M_1^2 - M_3^2)$, see eq. (2.4). Obviously, having all three masses different is a necessary, but not sufficient condition for CP violation. Any one of the neutral Higgs particles could be odd under CP, with the other two even. This would be reflected in a vanishing product $e_1 e_2 e_3$.

Properties of the Higgs boson observed at the LHC [41–43] match those expected for the SM. As has been discussed in [30, 44–46], the standard nature of the Higgs boson doesn't preclude the presence of interesting relatively low-scale BSM physics. This landscape is being referred to as the alignment limit. If we take the discovered 125 GeV Higgs boson to be the lightest one, H_1, then the alignment limit implies

$$e_1 \to v, \quad e_2 \to 0, \quad e_3 \to 0, \tag{6.1}$$

where $v = 246$ GeV. Hence, in this exact limit, $\mathrm{Im}\, J_2$ vanishes, and the CP-violating effects discussed in this paper, would all vanish. (Actually, also $\mathrm{Im}\, J_1$ would vanish.) In general, if we parametrize the deviation of the $H_1 VV$ coupling from its SM value by δ, such that $e_1 = v(1-\delta)$, then one can show that for small δ

$$|\mathrm{Im}\, J_2| < \frac{\delta}{v^6}(M_1^2 - M_2^2)(M_2^2 - M_3^2)(M_3^2 - M_1^2). \tag{6.2}$$

However, the scalar sector of the 2HDM might still offer CP violation in the alignment limit, represented by the remaining invariant $\mathrm{Im}\, J_{30}$ [30]. This quantity can only be accessed via measurements involving pairs of charged Higgs bosons, and is thus not easily studied. Thus, for the near future, the best prospects for finding CP violation in the 2HDM lie probably in these trilinear vector couplings, together with some deviation from the alignment limit [36, 37, 47, 48].

These effects of CP violation might be worth looking for also at the LHC, where in Drell-Yan processes a cut on rapidity makes it possible to statistically distinguish the quark from the antiquark direction [49]. An efficiency study might be worthwhile.

Of course, if an effect were to be found in ZZZ or ZW^+W^- trilinear couplings, at a level beyond that expected in the 2HDM, that would point to some other new physics.

Acknowledgments

It is a pleasure to thank professor W. Y. Keung and professor P. B. Pal for correspondence. BG thanks Jan Kalinowski for clarifying discussions and also acknowledges partial support by the National Science Centre (Poland) research project, decision no DEC-2014/13/B/ST2/03969. PO is supported in part by the Research Council of Norway.

A The ZZZ vertex

A.1 The HHH triangle diagram

We show in figure 12 the triangle diagram in LoopTools notation [35]. Treating all momenta p_1, $(-p_2)$ and $(-p_3)$ as incoming: $p_1 - p_2 - p_3 = 0$. Loop momenta along the three internal

JHEP05(2016)025

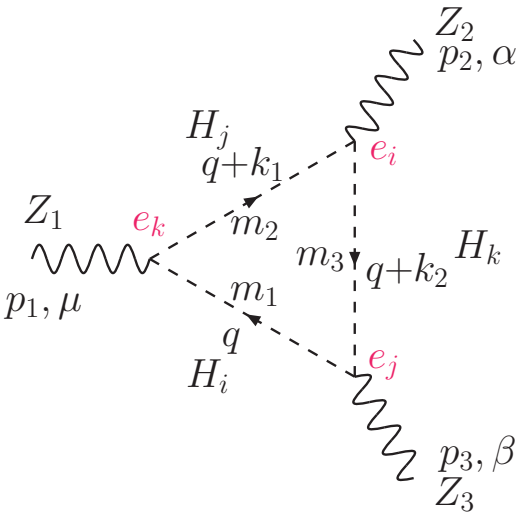

Figure 12. Triangle diagram contributing to the CP-violating ZZZ vertex.

lines are denoted q, $q+k_1$, $q+k_2$, whereas their masses are denoted m_1, m_2 and m_3 (some permutation of M_1, M_2, M_3).

Assuming that Z couples to light fermions we may drop terms proportional to p_1^μ, p_2^α and p_3^β. Furthermore, we assume that Z_2 and Z_3 are on-shell, meaning $p_2^2 = p_3^2 = M_Z^2$. Under these assumptions, the contribution to f_4^Z is given by the following sum over 6 permutations of i, j, k:

$$e\frac{p_1^2 - M_Z^2}{M_Z^2} f_4^{Z,HHH} = -8N_H e_1 e_2 e_3 \sum_{i,j,k} \epsilon_{ijk} C_{001}(p_1^2, M_Z^2, M_Z^2, M_i^2, M_j^2, M_k^2), \tag{A.1}$$

where

$$N_H = \frac{1}{16\pi^2}\left(\frac{g}{2v\cos\theta_W}\right)^3 = \frac{e\alpha}{4\pi v^3 \sin^3(2\theta_W)}. \tag{A.2}$$

A.2 The HHG triangle diagrams

In the covariant gauge, there are also contributions from triangle diagrams with one of the Higgs fields replaced by the Goldstone field G_0. A representative case is shown in figure 13. There are similar diagrams with a G_0 along either of the other two internal lines, but no diagram with two or three internal G_0 lines due to the non-existence of a ZG_0G_0 coupling.

We add these three sets of diagrams, summing over permutations of i, j, k and make the same assumptions as for the HHH triangle diagrams. We find that under these assumptions the remaining contribution to f_4^Z is given by

$$\begin{aligned} e\frac{p_1^2 - M_Z^2}{M_Z^2} f_4^{Z,HHG} = 8N_H e_1 e_2 e_3 \sum_{i,j,k} \epsilon_{ijk} \big[& C_{001}(p_1^2, M_Z^2, M_Z^2, M_i^2, M_j^2, M_Z^2) \\ & + C_{001}(p_1^2, M_Z^2, M_Z^2, M_Z^2, M_j^2, M_k^2) + C_{001}(p_1^2, M_Z^2, M_Z^2, M_i^2, M_Z^2, M_k^2) \big]. \end{aligned} \tag{A.3}$$

JHEP05(2016)025

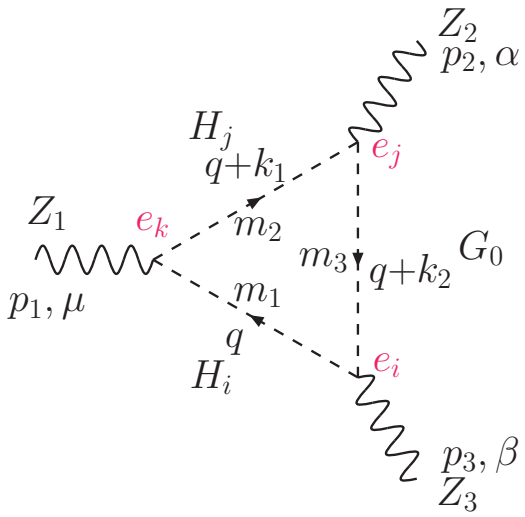

Figure 13. Triangle diagram contributing to the CP-violating ZZZ vertex.

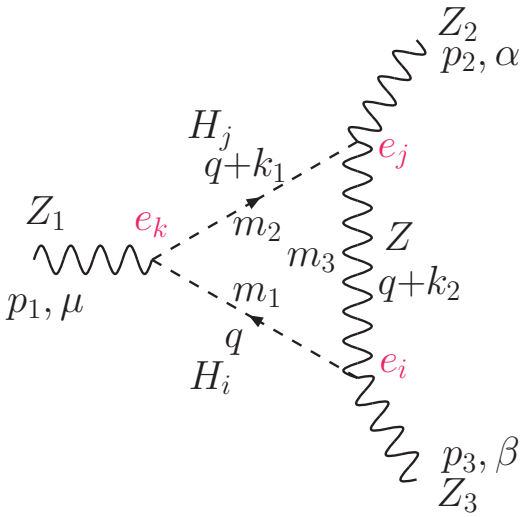

Figure 14. Triangle diagram contributing to the CP-violating ZZZ vertex.

A.3 The HHZ triangle diagrams

One of the lines in the triangle diagram could also be a Z, as indicated in figure 14. The Z-line can of course also be inserted between Z_3 and Z_1, or between Z_1 and Z_2, but there can not be more than one internal Z-line due to the absence of a tree-level ZZZ vertex. Again, we add these three sets of diagrams, summing over permutations of i, j, k and make the same assumptions as for the HHH and HHG triangle diagrams. We find that under these assumptions the remaining contribution to f_4^Z is given by

$$e\frac{p_1^2 - M_Z^2}{M_Z^2} f_4^{Z,HHZ} = 8M_Z^2 N_H e_1 e_2 e_3 \sum_{i,j,k} \epsilon_{ijk} C_1(p_1^2, M_Z^2, M_Z^2, M_i^2, M_Z^2, M_k^2). \tag{A.4}$$

JHEP05(2016)025

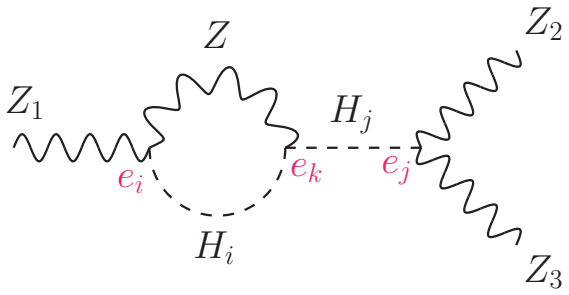

Figure 15. Bubble diagram contributing proportional to Im J_2.

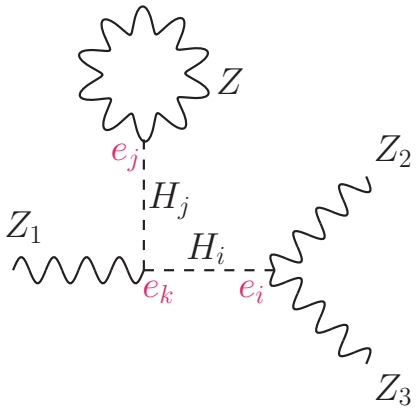

Figure 16. Tadpole diagram yielding a structure proportional to Im J_2.

A.4 Bubble diagrams

There are diagrams with a bubble connecting a Z_a $(a = 1, 2, 3)$ with an intermediate H_j, as shown in figure 15.

These diagrams contribute terms proportional to Im J_2. There are also diagrams with the internal Z replaced by a G_0. However, these diagrams are all scalar, proportional to $p_1^\mu g^{\alpha\beta}$ (and similarly for bubbles on the other legs) and will not be further discussed.

A.5 Tadpole diagrams

There are also tadpole diagrams yielding a structure proportional to Im J_2. A representative case is shown in figure 16. However, these are canceled by counter terms, in order to give a vanishing expectation value for the H_j field at the one-loop order [50].

B The ZW^+W^- vertex

Triangle diagrams of the kind shown in figure 17 contribute to the CP-violating ZW^+W^- vertex. In fact, they give a contribution proportional to the invariant Im J_2.

We show in figure 17 the triangle diagrams contributing to the CP-violating form factor in LoopTools notation [35]. The details of their calculations and the assumptions

JHEP05(2016)025

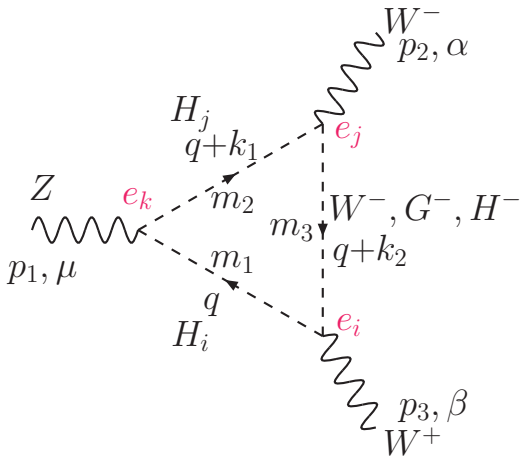

Figure 17. Triangle diagrams contributing to the CP-violating ZWW vertex.

made are similar to the calculations of the ZZZ vertex in the previous section, so we omit the details.

For those diagrams with a W^- line between W^+ and W^-, we find that their contribution is proportional to $p_1^\mu g^{\alpha\beta}$. We therefore neglect this contribution. Putting

$$N = \frac{-1}{16\pi^2 \cos\theta_{\rm W}} \left(\frac{g}{2v}\right)^3 = \frac{-e\alpha}{32\pi v^3 \cos\theta_{\rm W} \sin^3(\theta_{\rm W})}, \tag{B.1}$$

we find that for the diagrams with a G^- line between W^+ and W^-, their contribution is

$$ig_{ZWW}\Gamma^{\alpha\beta\mu}_{ZWW,HHG_{\rm ch}} = 8Ne_1e_2e_3(p_1^\alpha g^{\mu\beta} + p_1^\beta g^{\mu\alpha}) \sum_{i,j,k} \epsilon_{ijk} C_{001}(p_1^2, M_W^2, M_W^2, M_i^2, M_j^2, M_W^2). \tag{B.2}$$

As for the diagrams with an H^- line between W^+ and W^-, there are contributions to the CP-violating form factor as well as to CP-conserving ones. We present only the contribution to the CP-violating form factor, which becomes

$$\begin{aligned} ig_{ZWW}\Gamma^{\alpha\beta\mu}_{ZWW,HHH_{\rm ch}} = &-8Ne_1e_2e_3(p_1^\alpha g^{\mu\beta} + p_1^\beta g^{\mu\alpha}) \sum_{i,j,k} \epsilon_{ijk} C_{001}(p_1^2, M_W^2, M_W^2, M_i^2, M_j^2, M_{H^\pm}^2) \\ &+ \text{CP-conserving terms.} \end{aligned} \tag{B.3}$$

Furthermore, at the SM level, there are contributions from fermion loops. But these do not contribute to f_4^Z and will be ignored.

C Extracting Im J_2 — a case study

We have claimed in sections 3 and 4 that the contributions to f_4^Z from the diagrams studied in appendices A and B are proportional to Im J_2. However, Im J_2 is not explicit in the expressions (3.4) and (4.4). The expressions contain the factor $e_1e_2e_3$, but the factor $(M_1^2-M_2^2)(M_2^2-M_3^2)(M_3^2-M_1^2)$ is not explicitly visible. This remaining factor is "hidden"

JHEP05(2016)025

in the linear combination of C-functions. One readily finds numerically that the expressions for f_4^Z vanish whenever two of the scalars have the same mass, but extracting the "hidden" factor $(M_1^2 - M_2^2)(M_2^2 - M_3^2)(M_3^2 - M_1^2)$ analytically is not easily done. Making some assumptions makes this task easier.

Let us study the contribution from the triangle diagrams with $H_iH_jH_k$ in the loop. The contribution is presented in (A.1). Let us focus on the expression

$$\Sigma = \sum_{i,j,k} \epsilon_{ijk} C_{001}(p_1^2, M_Z^2, M_Z^2, M_i^2, M_j^2, M_k^2) \tag{C.1}$$

in the asymptotic limit (large $s_1 \equiv p_1^2$). The tensor coefficients C_{001} can all be re-expressed in terms of scalar loop integrals A_0, B_0 and C_0 [51]. The explicit forms of these scalar loop integrals are all known [52]. They can be expressed in terms of logarithms and dilogarithms. The resulting expression is very lengthy and complex, so we prepare to study the expression in the asymptotic limit by introducing new variables:

$$x = \frac{(M_2^2 - M_1^2)}{s_1} \tag{C.2}$$

$$y = \frac{(M_3^2 - M_2^2)}{s_1} \tag{C.3}$$

As a consequence,

$$x + y = \frac{(M_3^2 - M_1^2)}{s_1}, \tag{C.4}$$

and

$$\mathrm{Im}\, J_2 = 2\frac{e_1e_2e_3}{v^9} s_1^3 xy(x+y).$$

Both x and y are small in the asymptotic limit. Expanding Σ in power of x and y, we find that the leading term indeed contains the product $xy(x+y)$,

$$\begin{aligned} f_4^{Z,HHH} &= \frac{-2\alpha}{\pi \sin^3(2\theta_W)} \frac{M_Z^2}{p_1^2 - M_Z^2} \frac{e_1e_2e_3}{v^3} \sum_{i,j,k} \epsilon_{ijk} C_{001}(p_1^2, M_Z^2, M_Z^2, M_i^2, M_j^2, M_k^2) \\ &\simeq \frac{-\alpha}{4\pi \sin^3(2\theta_W)} \frac{v^6 M_Z^2}{M_1^2 s_1^2 (s_1 - M_Z^2)} \mathrm{Im} J_2 \\ &\quad \times \left(\log\left(\frac{M_1^2}{s_1}\right) + \frac{i\left(9M_1^2 - 2M_Z^2\right) \log\left(\frac{\sqrt{4M_1^2 - M_Z^2} - iM_Z}{\sqrt{4M_1^2 - M_Z^2} + iM_Z}\right)}{M_Z \sqrt{4M_1^2 - M_Z^2}} + i\pi \right) \end{aligned}$$

in the asymptotic limit. Here, both M_2^2 and M_3^2 have been represented by M_1^2, since $x \ll 1$ and $y \ll 1$.

D Some asymmetry prefactors $\mathcal{F}$

D.1 The prefactor $\mathcal{F}_1(\beta, \Theta)$ of $\mathcal{A}_1^{ZZ}$

We define the prefactor of eq. (5.4) as

$$\mathcal{F}_1(\beta, \Theta) = \frac{N_0 + N_1 \cos\Theta + N_2 \cos^2\Theta + N_3 \cos^3\Theta}{D_0 + D_1 \cos\Theta + D_2 \cos^2\Theta + D_3 \cos^3\Theta + D_4 \cos^4\Theta}. \tag{D.1}$$

JHEP05(2016)025

These coefficients are given by

$$N_0 = \left(1+\beta^2\right)\xi_1, \qquad N_1 = -2\beta^2\left(\xi_1-\xi_2\right), \tag{D.2a}$$

$$N_2 = \left(\beta^2-3\right)\xi_1, \qquad N_3 = 2\left(\xi_1-\xi_2\right), \tag{D.2b}$$

$$D_0 = \left(1+\beta^2\right)^2\left(\xi_3+\xi_4\right), \qquad D_1 = 2\left(1-\beta^4\right)\xi_3, \tag{D.2c}$$

$$D_2 = -\left(3+6\beta^2-\beta^4\right)\left(\xi_3+\xi_4\right), \qquad D_3 = -4\left(1-\beta^2\right)\xi_3, \tag{D.2d}$$

$$D_4 = 4\left(\xi_3+\xi_4\right), \tag{D.2e}$$

with

$$\xi_1 = \sin\theta_W\cos\theta_W(1-6\sin^2\theta_W+12\sin^4\theta_W), \tag{D.3a}$$

$$\xi_2 = 16\sin^7\theta_W\cos\theta_W, \tag{D.3b}$$

$$\xi_3 = 1-8\sin^2\theta_W+24\sin^4\theta_W-32\sin^6\theta_W, \tag{D.3c}$$

$$\xi_4 = 32\sin^8\theta_W. \tag{D.3d}$$

D.2 The prefactor $\mathcal{F}(s_1,\Theta)$ of $\mathcal{A}^{ud}$

The prefactor of the asymmetry $\mathcal{A}^{ud}$ of eq. (5.28) can be written as

$$\mathcal{F}(s_1,\Theta) = \frac{N_0^{ud}+N_1^{ud}\cos\Theta+N_2^{ud}\cos^2\Theta}{D_0^{ud}+D_1^{ud}\cos\Theta+D_2^{ud}\cos^2\Theta+D_3^{ud}\cos^3\Theta+D_4^{ud}\cos^4\Theta} \tag{D.4}$$

with

$$N_0^{ud} = \left(1-\beta^2\right)\left(1-2\sin^2\theta_W\right)\left(s_1-m_Z^2\right), \tag{D.5a}$$

$$N_1^{ud} = \beta\left[\left(1-\beta^2\right)\left(1-2\sin^2\theta_W\right)s_1 - \left(2-2\left(3+\beta^2\right)\sin^2\theta_W+8\left(1+\beta^2\right)\sin^4\theta_W\right)m_Z^2\right], \tag{D.5b}$$

$$N_2^{ud} = 2\beta^2\left(1-4\sin^2\theta_W+8\sin^4\theta_W\right)m_Z^2, \tag{D.5c}$$

and

$$\begin{aligned} D_0^{ud} = &-\left(1-\beta^2\right)^2\left(16+11\beta^2-18\beta^4+3\beta^6\right)s_1^2 \\ &+4\left(1-\beta^2\right)\left(8+7\beta^2-14\beta^4+3\beta^6-\beta^2\left(19+\beta^2-15\beta^4+3\beta^6\right)\sin^2\theta_W\right)m_Z^2 s_1 \\ &-4\left(4+9\beta^2-10\beta^4+\beta^6-2\beta^2\left(19+\beta^2-15\beta^4+3\beta^6\right)\sin^2\theta_W\right. \\ &\left.+2\beta^2\left(1+\beta^2\right)^2\left(19-18\beta^2+3\beta^4\right)\sin^4\theta_W\right)m_Z^4, \end{aligned} \tag{D.6a}$$

$$\begin{aligned} D_1^{ud} = 4\beta\Big[&\left(1-\beta^2\right)^2\left(8-9\beta^2+3\beta^4\right)s_1^2 \\ &-4\left(1-\beta^2\right)\left(6-4\beta^2-\left(4+9\beta^2-12\beta^4+3\beta^6\right)\sin^2\theta_W\right)m_Z^2 s_1 \\ &+4\left(4+\beta^2-3\beta^4-4\left(1+6\beta^2-5\beta^4\right)\sin^2\theta_W\right. \\ &\left.+2\beta^2\left(19+\beta^2-15\beta^4+3\beta^6\right)\sin^4\theta_W\right)m_Z^4\Big], \end{aligned} \tag{D.6b}$$

$$\begin{aligned} D_2^{ud} = \beta^2\left(1-\beta^2\right)\Big[&\left(1-\beta^2\right)^2\left(11-3\beta^2\right)s_1^2 \\ &+4\left(1-\beta^2\right)\left(3\left(3+\beta^2\right)-\left(29-8\beta^2+3\beta^4\right)\sin^2\theta_W\right)m_Z^2 s_1 \\ &-4\left(11+5\beta^2-\left(26+32\beta^2+6\beta^4\right)\sin^2\theta_W\right. \\ &\left.-\left(6-138\beta^2+10\beta^4-6\beta^6\right)\sin^4\theta_W\right)m_Z^4\Big], \end{aligned} \tag{D.6c}$$

JHEP05(2016)025

$$D_3^{ud} = 4\beta^3 \Big[\left(1-\beta^2\right)^2 \left(1-3\beta^2\right) s_1^2 + 4\left(1-\beta^2\right)\left(2\beta^2 - \left(1+3\beta^4\right)\sin^2\theta_W\right) m_Z^2 s_1 \\ - 4\left(1+\beta^2 - 4\left(1+\beta^4\right)\sin^2\theta_W \right. \\ \left. + \left(6+2\beta^2+2\beta^4+6\beta^6\right)\sin^4\theta_W\right) m_Z^4 \Big], \tag{D.6d}$$

$$D_4^{ud} = 4\beta^4 \Big(3\left(1-\beta^2\right)^2 s_1^2 - 4\left(1-\beta^2\right)\left(1+\left(1-3\beta^2\right)\sin^2\theta_W\right) m_Z^2 s_1 \\ +4\left(1-2\left(1+\beta^2\right)\sin^2\theta_W + \left(6-4\beta^2+6\beta^4\right)\sin^4\theta_W\right) m_Z^4 \Big). \tag{D.6e}$$

At high energies ($s_1 \gg M_Z^2$), the prefactor grows as γ^2. In the perpendicular direction, $\cos\Theta \to 0$, it takes the form

$$\mathcal{F}(s_1,\Theta) \to -\frac{\gamma^2 M_W^4 (2M_W^2 - M_Z^2)}{M_Z^2(12M_W^4 - 8M_W^2 M_Z^2 + 5M_Z^4)}, \tag{D.7}$$

whereas in the forward direction it is more singular. That singularity is however tamed by the other factors of eq. (5.28).

D.3 The prefactors $\mathcal{F}^{WW}$ and $\tilde{\mathcal{F}}^{WW}$ of A^{WW} and $\tilde{A}^{WW}$

We define

$$\mathcal{F}^{WW} \equiv \frac{(N_0 + N_1\cos\Theta + N_2\cos^2\Theta)s_1}{D_0 + D_1\cos\Theta + D_2\cos^2\Theta + D_3\cos^3\Theta + D_4\cos^4\Theta}, \tag{D.8}$$

and

$$\tilde{\mathcal{F}}^{WW} \equiv \frac{(\tilde{N}_0 + \tilde{N}_1\cos\Theta + \tilde{N}_2\cos^2\Theta + \tilde{N}_3\cos^3\Theta)s_1}{D_0 + D_1\cos\Theta + D_2\cos^2\Theta + D_3\cos^3\Theta + D_4\cos^4\Theta}. \tag{D.9}$$

The coefficients are given by

$$N_0 = \left(1-\beta^2\right)\left(1-2\sin^2\theta_W\right)\left(s_1 - m_Z^2\right), \tag{D.10a}$$
$$N_1 = 2\beta\left[\left(1-\beta^2\right)\left(1-2\sin^2\theta_W\right)s_1 - 2\left(1-\left(3+\beta^2\right)\sin^2\theta_W\right)m_Z^2\right], \tag{D.10b}$$
$$N_2 = -3\left(1-\beta^2\right)\left(1-2\sin^2\theta_W\right)s_1 + \left(3+\beta^2-\left(6+10\beta^2\right)\sin^2\theta_W\right)m_Z^2, \tag{D.10c}$$
$$\tilde{N}_0 = -\beta\left(1-\beta^2\right)\left(1-2\sin^2\theta_W\right)s_1 \\ + 2\beta\left(1-\left(3+\beta^2\right)\sin^2\theta_W + 4\left(1+\beta^2\right)\sin^4\theta_W\right)m_Z^2, \tag{D.10d}$$
$$\tilde{N}_1 = -2\beta^2\left(1-4\sin^2\theta_W + 8\sin^4\theta_W\right)m_Z^2, \tag{D.10e}$$
$$\tilde{N}_2 = -\beta\left[\left(1-\beta^2\right)\left(1-2\sin^2\theta_W\right)s_1 \right. \\ \left. - \left(2-2\left(3+\beta^2\right)\sin^2\theta_W + 8\left(1+\beta^2\right)\sin^4\theta_W\right)m_Z^2\right], \tag{D.10f}$$
$$\tilde{N}_3 = 2\left(1-\beta^2\right)\left(1-2\sin^2\theta_W\right)s_1 - 2\left(1-2\left(1+\beta^2\right)\sin^2\theta_W + 8\beta^2\sin^4\theta_W\right)m_Z^2, \tag{D.10g}$$

JHEP05(2016)025

and

$$D_0 = \left(1+\beta^2\right)\Big[\left(1-\beta^2\right)^2 s_1^2 - 2\left(1-\beta^2\right)\left(1-2\beta^2\sin^2\theta_W\right) m_Z^2 s_1 + \left(1+\beta^2-8\beta^2\sin^2\theta_W+8\beta^2\left(1+\beta^2\right)\sin^4\theta_W\right) m_Z^4\Big], \tag{D.11a}$$

$$D_1 = 4\beta^3 m_Z^2\left[\left(1-\beta^2\right)\left(1-2\sin^2\theta_W\right) s_1 - \left(2-2\left(3+\beta^2\right)\sin^2\theta_W+8\left(1+\beta^2\right)\sin^4\theta_W\right) m_Z^2\right], \tag{D.11b}$$

$$D_2 = -\left(3-\beta^2\right)\left(1-\beta^2\right)^2 s_1^2 + 2\left(3-8\beta^2+5\beta^4+2\beta^2\left(1-\beta^4\right)\sin^2\theta_W\right) m_Z^2 s_1 - \left(3-10\beta^2-\beta^4+8\beta^2\left(1+3\beta^2\right)\sin^2\theta_W-8\beta^2\left(1+6\beta^2+\beta^4\right)\sin^4\theta_W\right) m_Z^4, \tag{D.11c}$$

$$D_3 = -4\beta\Big[\left(1-\beta^2\right)^2 s_1^2 - \left(1-\beta^2\right)\left(3-\left(2+4\beta^2\right)\sin^2\theta_W\right) m_Z^2 s_1 + \left(2-2\left(1+3\beta^2\right)\sin^2\theta_W+8\beta^2\left(1+\beta^2\right)\sin^4\theta_W\right) m_Z^4\Big], \tag{D.11d}$$

$$D_4 = 4\left(1-\beta^2\right)^2 s_1^2 - 8\left(1-\beta^2\right)\left(1-2\beta^2\sin^2\theta_W\right) m_Z^2 s_1 + 4\left(1-4\beta^2\sin^2\theta_W+8\beta^4\sin^4\theta_W\right) m_Z^4. \tag{D.11e}$$

Open Access. This article is distributed under the terms of the Creative Commons Attribution License (CC-BY 4.0), which permits any use, distribution and reproduction in any medium, provided the original author(s) and source are credited.

References

[1] K.J.F. Gaemers and G.J. Gounaris, *Polarization Amplitudes for $e^+e^- \to W^+W^-$ and $e^+e^- \to ZZ$*, *Z. Phys.* **C 1** (1979) 259 [INSPIRE].

[2] K. Hagiwara, R.D. Peccei, D. Zeppenfeld and K. Hikasa, *Probing the Weak Boson Sector in $e^+e^- \to W^+W^-$*, *Nucl. Phys.* **B 282** (1987) 253 [INSPIRE].

[3] G.J. Gounaris, J. Layssac and F.M. Renard, *Signatures of the anomalous $Z\gamma$ and ZZ production at the lepton and hadron colliders*, *Phys. Rev.* **D 61** (2000) 073013 [hep-ph/9910395] [INSPIRE].

[4] G.J. Gounaris, J. Layssac and F.M. Renard, *Off-shell structure of the anomalous Z and γ selfcouplings*, *Phys. Rev.* **D 62** (2000) 073012 [hep-ph/0005269] [INSPIRE].

[5] U. Baur and D.L. Rainwater, *Probing neutral gauge boson selfinteractions in ZZ production at hadron colliders*, *Phys. Rev.* **D 62** (2000) 113011 [hep-ph/0008063] [INSPIRE].

[6] ALEPH, DELPHI, L3, OPAL and LEP Electroweak collaborations, S. Schael et al., *Electroweak Measurements in Electron-Positron Collisions at W-Boson-Pair Energies at LEP*, *Phys. Rept.* **532** (2013) 119 [arXiv:1302.3415] [INSPIRE].

[7] CDF collaboration, T. Aaltonen et al., *First Measurement of ZZ Production in $p\bar{p}$ Collisions at $\sqrt{s} = 1.96$-TeV*, *Phys. Rev. Lett.* **100** (2008) 201801 [arXiv:0801.4806] [INSPIRE].

[8] CDF collaboration, T. Aaltonen et al., *First Observation of Vector Boson Pairs in a Hadronic Final State at the Tevatron Collider*, *Phys. Rev. Lett.* **103** (2009) 091803 [arXiv:0905.4714] [INSPIRE].

[9] D0 collaboration, V.M. Abazov et al., *Measurement of the ZZ production cross section in $p\bar{p}$ collisions at $\sqrt{s} = 1.96$ TeV*, *Phys. Rev.* **D 84** (2011) 011103 [arXiv:1104.3078] [INSPIRE].

JHEP05(2016)025

[10] D0 collaboration, V.M. Abazov et al., *A measurement of the WZ and ZZ production cross sections using leptonic final states in 8.6 fb^{-1} of $p\bar{p}$ collisions*, *Phys. Rev.* **D 85** (2012) 112005 [arXiv:1201.5652] [INSPIRE].

[11] ATLAS collaboration, *Measurement of the ZZ production cross section and limits on anomalous neutral triple gauge couplings in proton-proton collisions at $\sqrt{s} = 7$ TeV with the ATLAS detector*, *Phys. Rev. Lett.* **108** (2012) 041804 [arXiv:1110.5016] [INSPIRE].

[12] CMS collaboration, *Measurement of the ZZ production cross section and search for anomalous couplings in 2l2l' final states in pp collisions at $\sqrt{s} = 7$ TeV*, *JHEP* **01** (2013) 063 [arXiv:1211.4890] [INSPIRE].

[13] ATLAS collaboration, *Measurement of ZZ production in pp collisions at $\sqrt{s} = 7$ TeV and limits on anomalous ZZZ and $ZZ\gamma$ couplings with the ATLAS detector*, *JHEP* **03** (2013) 128 [arXiv:1211.6096] [INSPIRE].

[14] N. Edwards, *Measurement of the ZZ production cross section and limits on anomalous neutral triple gauge couplings with the ATLAS detector*, Ph.D. Thesis, Glasgow University, (2013).

[15] K.D. Gregersen, *Anomalous trilinear gauge couplings in ZZ production at the ATLAS experiment*, Ph.D. Thesis, NBI, University of Copenhagen, (2013), CERN-THESIS-2013-338.

[16] ATLAS collaboration, *Measurement of the total ZZ production cross section in proton-proton collisions at $\sqrt{s} = 8$ TeV in 20 fb^{-1} with the ATLAS detector*, ATLAS-CONF-2013-020 (2013).

[17] CMS collaboration, *Measurement of the W^+W^- Cross section in pp Collisions at $\sqrt{s} = 7$ TeV and Limits on Anomalous $WW\gamma$ and WWZ couplings*, *Eur. Phys. J.* **C 73** (2013) 2610 [arXiv:1306.1126] [INSPIRE].

[18] CMS collaboration, *Measurement of the $pp \to ZZ$ production cross section and constraints on anomalous triple gauge couplings in four-lepton final states at $\sqrt{s} = 8$ TeV*, *Phys. Lett.* **B 740** (2015) 250 [arXiv:1406.0113] [INSPIRE].

[19] ATLAS collaboration, *Measurement of the $WW + WZ$ cross section and limits on anomalous triple gauge couplings using final states with one lepton, missing transverse momentum and two jets with the ATLAS detector at $\sqrt{s} = 7$ TeV*, *JHEP* **01** (2015) 049 [arXiv:1410.7238] [INSPIRE].

[20] CMS collaboration, *Measurements of the ZZ production cross sections in the 2l2ν channel in proton-proton collisions at $\sqrt{s} = 7$ and 8 TeV and combined constraints on triple gauge couplings*, *Eur. Phys. J.* **C 75** (2015) 511 [arXiv:1503.05467] [INSPIRE].

[21] CMS collaboration, *Measurement of the W^+W^- cross section in pp collisions at $\sqrt{s} = 8$ TeV and limits on anomalous gauge couplings*, arXiv:1507.03268 [INSPIRE].

[22] T.D. Lee, *A Theory of Spontaneous T Violation*, *Phys. Rev.* **D 8** (1973) 1226 [INSPIRE].

[23] L. Lavoura and J.P. Silva, *Fundamental CP-violating quantities in a SU(2) × U(1) model with many Higgs doublets*, *Phys. Rev.* **D 50** (1994) 4619 [hep-ph/9404276] [INSPIRE].

[24] F.J. Botella and J.P. Silva, *Jarlskog-like invariants for theories with scalars and fermions*, *Phys. Rev.* **D 51** (1995) 3870 [hep-ph/9411288] [INSPIRE].

[25] J.F. Gunion and H.E. Haber, *Conditions for CP-violation in the general two-Higgs-doublet model*, *Phys. Rev.* **D 72** (2005) 095002 [hep-ph/0506227] [INSPIRE].

JHEP05(2016)025

[26] G.C. Branco, M.N. Rebelo and J.I. Silva-Marcos, *CP-odd invariants in models with several Higgs doublets*, *Phys. Lett.* **B 614** (2005) 187 [hep-ph/0502118] [INSPIRE].

[27] S. Davidson and H.E. Haber, *Basis-independent methods for the two-Higgs-doublet model*, *Phys. Rev.* **D 72** (2005) 035004 [*Erratum ibid.* **D 72** (2005) 099902] [hep-ph/0504050] [INSPIRE].

[28] A. Denner and T. Sack, *Electroweak Radiative Corrections To $e^+e^- \to Z^0Z^0$*, *Nucl. Phys.* **B 306** (1988) 221 [INSPIRE].

[29] M. Böhm, A. Denner, T. Sack, W. Beenakker, F.A. Berends and H. Kuijf, *Electroweak Radiative Corrections to $e^+e^- \to W^+W^-$*, *Nucl. Phys.* **B 304** (1988) 463 [INSPIRE].

[30] B. Grzadkowski, O.M. Ogreid and P. Osland, *Measuring CP-violation in Two-Higgs-Doublet models in light of the LHC Higgs data*, *JHEP* **11** (2014) 084 [arXiv:1409.7265] [INSPIRE].

[31] X.G. He, J.P. Ma and B.H.J. McKellar, *CP violating form-factors for three gauge boson vertex in the two Higgs doublet and left-right symmetric models*, *Phys. Lett.* **B 304** (1993) 285 [hep-ph/9209260] [INSPIRE].

[32] D. Chang, W.-Y. Keung and P.B. Pal, *CP violation in the cubic coupling of neutral gauge bosons*, *Phys. Rev.* **D 51** (1995) 1326 [hep-ph/9407294] [INSPIRE].

[33] D. Chang, W.-Y. Keung and I. Phillips, *CP violating observables in $e^-e^+ \to W^-W^+$*, *Phys. Rev.* **D 48** (1993) 4045 [hep-ph/9307232] [INSPIRE].

[34] J.F. Nieves and P.B. Pal, *Electromagnetic properties of neutral and charged spin 1 particles*, *Phys. Rev.* **D 55** (1997) 3118 [hep-ph/9611431] [INSPIRE].

[35] T. Hahn and M. Pérez-Victoria, *Automatized one loop calculations in four-dimensions and D-dimensions*, *Comput. Phys. Commun.* **118** (1999) 153 [hep-ph/9807565] [INSPIRE].

[36] L. Basso et al., *Probing the charged Higgs boson at the LHC in the CP-violating type-II 2HDM*, *JHEP* **11** (2012) 011 [arXiv:1205.6569] [INSPIRE].

[37] L. Basso et al., *The CP-violating type-II 2HDM and Charged Higgs boson benchmarks*, arXiv:1305.3219 [INSPIRE].

[38] ILC collaboration, G. Aarons et al., *International Linear Collider Reference Design Report Volume 2: Physics at the ILC*, arXiv:0709.1893 [INSPIRE].

[39] P. Lebrun et al., *The CLIC Programme: Towards a Staged e^+e^- Linear Collider Exploring the Terascale: CLIC Conceptual Design Report*, arXiv:1209.2543 [INSPIRE].

[40] G. Gounaris, D. Schildknecht and F.M. Renard, *Genuine tests of CP invariance in $e^+e^- \to W^+W^-$*, *Phys. Lett.* **B 263** (1991) 291 [INSPIRE].

[41] CMS collaboration, *Constraints on the spin-parity and anomalous HVV couplings of the Higgs boson in proton collisions at 7 and 8 TeV*, *Phys. Rev.* **D 92** (2015) 012004 [arXiv:1411.3441] [INSPIRE].

[42] CMS collaboration, *Precise determination of the mass of the Higgs boson and tests of compatibility of its couplings with the standard model predictions using proton collisions at 7 and 8 TeV*, *Eur. Phys. J.* **C 75** (2015) 212 [arXiv:1412.8662] [INSPIRE].

[43] ATLAS collaboration, *Study of the spin and parity of the Higgs boson in diboson decays with the ATLAS detector*, *Eur. Phys. J.* **C 75** (2015) 476 [arXiv:1506.05669] [INSPIRE].

[44] J.F. Gunion and H.E. Haber, *The CP conserving two Higgs doublet model: The Approach to the decoupling limit*, *Phys. Rev.* **D 67** (2003) 075019 [hep-ph/0207010] [INSPIRE].

JHEP05(2016)025

[45] P.S. Bhupal Dev and A. Pilaftsis, *Maximally Symmetric Two Higgs Doublet Model with Natural Standard Model Alignment*, *JHEP* **12** (2014) 024 [*Erratum ibid.* **11** (2015) 147] [arXiv:1408.3405] [INSPIRE].

[46] J. Bernon, J.F. Gunion, H.E. Haber, Y. Jiang and S. Kraml, *Scrutinizing the alignment limit in two-Higgs-doublet models: $m_h = 125$ GeV*, *Phys. Rev.* **D 92** (2015) 075004 [arXiv:1507.00933] [INSPIRE].

[47] D. Fontes, J.C. Romão, R. Santos and J.P. Silva, *Large pseudoscalar Yukawa couplings in the complex 2HDM*, *JHEP* **06** (2015) 060 [arXiv:1502.01720] [INSPIRE].

[48] D. Fontes, J.C. Romão, R. Santos and J.P. Silva, *Undoubtable signs of CP-violation in Higgs boson decays at the LHC run 2*, *Phys. Rev.* **D 92** (2015) 055014 [arXiv:1506.06755] [INSPIRE].

[49] M. Dittmar, *Neutral current interference in the TeV region: The Experimental sensitivity at the LHC*, *Phys. Rev.* **D 55** (1997) 161 [hep-ex/9606002] [INSPIRE].

[50] R. Santos and A. Barroso, *On the renormalization of two Higgs doublet models*, *Phys. Rev.* **D 56** (1997) 5366 [hep-ph/9701257] [INSPIRE].

[51] A. Denner and S. Dittmaier, *Reduction of one loop tensor five point integrals*, *Nucl. Phys.* **B 658** (2003) 175 [hep-ph/0212259] [INSPIRE].

[52] A. Denner, *Techniques for calculation of electroweak radiative corrections at the one loop level and results for W-physics at LEP 200*, *Fortsch. Phys.* **41** (1993) 307 [arXiv:0709.1075] [INSPIRE].

JHEP05(2016)025